Non-bonding pairs in cyclic thioethers: Electrostatic modelling and *ab initio* calculations for complexes of 2,5-dihydrothiophene, thietane and thiirane with hydrogen fluoride

J. Grant Hill[1] and Anthony C. Legon[2]

[1]Department of Chemistry, University of Sheffield, Sheffield S3 7HF, U.K., grant.hill@sheffield.ac.uk

[2]School of Chemistry, University of Bristol, Cantock's Close, Bristol BS8 1TS, U.K., a.c.legon@bristol.ac.uk

Abstract.

Locations of nucleophilic regions of Lewis bases play important roles in the geometry of intermolecular complexes and can be probed by small molecules with an electrophilic region (e.g. HF). The electrostatic potential energy $V(\phi)$ of a non-perturbing, protonic charge at a fixed distance r from the S atom in three cyclic thioethers was examined as a function of the angle ϕ made by the $\textbf{\textit{r}}$-vector with the C_2 axis (in thiirane and 2,5-dihydrothiophene) or the local C_2 axis associated with the C–S–C plane of the thietane ring. The electrostatic PE $V_{\text{HF}}(\phi)$ of HF, when HF is modelled as an extended electric dipole, was also calculated as a function of ϕ and the results compared with the geometries of the complexes thiirane···HF, thietane···HF and 2,5-dihydrothiophene···HF calculated at the CCSD(T)-F12c/cc-pVTZ-F12 level. The calculations reveal angular deviations $\theta \sim 10\text{-}20°$ of the S···H–F nuclei from collinearity in a direction suggesting secondary interactions of the nucleophilic region of F with electrophilic H atom(s) of the rings. They also reveal the angles ϕ made by the S···H hydrogen bond with the C_2 (or local C_2) axes in the thioether···HF complexes are systematically larger ($\sim 4\text{-}9°$) than those at the minima in the $V_{\text{HF}}(\phi)$ functions, but the latter do agree with the directions of maximum nucleophilicity shown by MESP diagrams of the thioethers. The deviation between these geometries can be explained with a simple model for complex formation. In the simple electrostatic model, the minima $|\phi_{\text{min}}|$ in the $V(\phi)$ versus ϕ functions occur at values smaller ($\sim 5\text{-}10°$) than those in the $V_{\text{HF}}(\phi)$ curves.

1. Introduction.

Non-covalent interactions perform a vital role in numerous chemical and biological processes, from small gas-phase complexes through to the structure, dynamics and activity of macromolecules, including DNA. Several of these non-covalent interactions, including the hydrogen bond and the halogen bond, have been

formally defined by IUPAC working parties,[1,2] and simple models can be applied to account for the bond. The basis of the simple model is that an electrophilic region of the molecule or functional group acting as a Lewis acid (the hydrogen atom in a hydrogen bond, or the halogen atom in a halogen bond) interacts with the nucleophilic region of a Lewis base B (typically non-bonding or π-bonding electron pairs). The terminology σ-hole or π-hole is often attached to the electrophilic region,[3,4] and the simple models provide an almost intuitive methodology for predictions of the angular geometries of supramolecular complexes. It is important to note that simple models typically sacrifice some of the subtleties of the underlying nature of the interactions, which has led to great and occasionally heated debate surrounding, for example, the role of charge transfer / degree of covalency within these bonds.[5–11]

The relative orientations of hydrogen-bonded complexes in the gas-phase has been the subject of a number of systematic studies, both experimentally (by microwave and infrared spectroscopy) and theoretically, see refs. 9,12–14, for examples and further references. In particular, the use of hydrogen fluoride as a probe molecule has allowed for explorations of the nucleophilic regions of Lewis bases that act as hydrogen bond acceptors. Extending the choice of probe molecules to encompass HX, where X is a halogen atom, CN group or C≡CH, led to the formulation of simple rules for gas-phase geometries of complexes.[12,13] A key component of these geometries is the directionality of the interaction, which can be expressed in terms of the angle ϕ (see Figure 1). These angular geometry prediction rules have been demonstrated to be electrostatic in origin and thus can be tested by careful examination of the electrostatic potential, and its angular dependence, in the region surrounding the atom or centre of the Lewis base directly involved in the hydrogen or halogen bond.[13] Similar arguments apply to the Lewis acid partner in the complex, and logically the sensitivity of the strength of the interaction to the directionality has been linked to the location (or absence of) non-bonding electron pairs in the valence shell of the hydrogen or halogen in the Lewis acid.[15]

One of the most suitable Lewis bases to consider in terms of the angular dependence of the electrostatic potential is the water molecule. Water and its congener hydrogen sulphide form hydrogen-bonded complexes $H_2O\cdots HX$[16–22] and $H_2S\cdots HX$[23–27] with the hydrogen halides HX (X =F, Cl, Br, I) in the gas phase. They have all been investigated by means of their rotational spectra. Of these, only $H_2O\cdots HF$ could be detected in equilibrium gas mixtures of water and the hydrogen halide at moderately low temperatures (~ 200 K), under which conditions vibrational satellites associated with low-frequency intermolecular modes were observed. The satellites correspond to the same rotational transition but in vibrationally excited states and their analysis allowed, *inter alia*, the potential energy function associated with the low-frequency intermolecular bending mode to be determined.[18] This function, which is shown in Figure 1(a) (blue curve and labels) together with energy levels of the low frequency, intermolecular bending mode deduced from it, is of the double-minimum type having a low barrier at the planar configuration and two minima

corresponding to equivalent pyramidal arrangements at O. The barrier to inversion lies below the zero-point energy level of the molecule. Thus, although the configuration at O is pyramidal at equilibrium, the molecule is effectively planar in the zero-point state (i.e. the vibrational wavefunctions have C_{2v} symmetry). The separation between the $v = 0$ and 1 states associated with the inversion mode is large relative to rotational energy level spacings. Other molecules $H_2O\cdots HX$[19–22] were studied in the vibrational ground state by pulsed-jet, Fourier-transform microwave spectroscopy, but the equilibrium geometry was deduced by various observations to be again pyramidal at O, with a low barrier to inversion, as confirmed by *ab initio* calculations. A similar conclusion obtains for several halogen-bonded complexes $H_2O\cdots XY$[28–34] (XY is a homo- or hetero-nuclear di-halogen molecule). Equilibrium values ϕ_e were estimated to lie in the range 35-55° from the rotational constants of each $H_2O\cdots HX$ and $H_2O\cdots XY$ investigated

The situation for $H_2S\cdots HX$ complexes is quite different.[23–27] Although studied only in the zero-point vibrational state in a supersonic expansion at ~ 2 K, it was possible to deduce that the configuration at S is rigidly pyramidal on the microwave timescale in all but one case, with undetectable inversion splitting between the zero-point state and the first vibrationally excited state and therefore a high barrier to the inversion motion. This conclusion was again confirmed by *ab initio* calculations. The exception was $H_2S\cdots HI$,[27] which also exhibited a rotational spectrum in a low-lying vibrationally excited state even at ~ 2 K and therefore showed evidence of conformational non-rigidity. Angles ϕ_e were found to be close to 90° in all other cases investigated. Similar results, with $\phi_e \sim 90°$ and conformational rigidity, were established for several halogen-bonded complexes $H_2S\cdots XY$.[35–40]

The different experimental conclusions for $H_2O\cdots HX$ and $H_2S\cdots HX$ complexes suggest that the equilibrium conformations can be predicted by assuming that in the equilibrium geometry the HX molecule lies along the axis of one of the non-bonding (n) electron pairs carried by O or S.[12,13] The model commonly used by chemists invokes sp^3 hybridisation at O in H_2O, with the half-angle of $\sim 50°$ between two equivalent n-pairs, as shown in Figure 2 in the schematic, exaggerated form commonly employed in chemistry. For H_2S, the S–H bonds can be understood if each H 1s orbital overlaps with one of the two orthogonal p orbital on S (hence an angle HSH $\sim 90°$) and if two sp hybrid orbitals at 180° contain one n-pair each (see Figure 2). This model can be validated by calculating the electrostatic potential energy of a non-perturbing, positive charge maintained at a fixed distance r from S. Figures 1 and 2 show the results for $V(\phi)$ as a function of ϕ, the angle made by a protonic charge with the plane of the three H_2Z nuclei (Z = O and S, respectively), when $r =1.74$ Å (the O$\cdots$H distance in $H_2O\cdots HF$)[13] and 2.31 Å (the S$\cdots$H distance in $H_2S\cdots HF$)[13], respectively, and when r is confined to the plane perpendicular to the nuclear plane.[13] The electric charge distribution employed for H_2O was determined by using the CCSD/cc-pV5Z wavefunction. Figure 2 displays two such $V(\phi)$ versus ϕ curves for H_2S. The blue curve results from a distributed multipole analysis (DMA) carried out by Buckingham and Fowler[41] using a wavefunction calculated at the SCF level with

large basis sets. Also shown in Figure 2 is the potential energy curve (red) recalculated by using the DMA of H_2S obtained from a CCSD/cc-pV(5+d)Z wavefunction. The difference between the two curves in Figure 2 is very small. The two minima at $\phi \simeq \pm 80°$ seen in Figure 2 clearly correspond with the most nucleophilic regions of H_2S and the two n-pair directions. The corresponding diagram for H_2O exhibits two minima at $\phi \simeq \pm 30°$. This methodology of probing the electrostatic potential of molecules with a view to predicting and understanding how intermolecular interactions may form is thus complementary to other techniques such as visualising the non-covalent interactions index (NCI).[42,43]

A more sophisticated model of $H_2O \cdots HX$, for example, involves a non-perturbing, extended electric dipole moment μ to represent HX, rather than a unit positive charge. HF can be represented as two point charges $\delta+$ and $\delta-$ separated by the HF bond length, with δ chosen from the DMA in ref. 41. The resulting potential energy $V(\phi)$ for $H_2O \cdots HF$ calculated at the appropriate distance $r(O \cdots H)$ is shown in blue as curve (c) in Figure 1 and is close to that [curve (a)] determined from experiment, with minima at $\phi \simeq \pm 55°$. This value of ϕ_{min} is encompassed by the experimental value[18] [$\pm 46(8)°$] and is consistent with tetrahedrally disposed n-pairs on O.[13] The barrier height (2.9 kJ mol^{-1}) for curve (c) in Figure 1 is also similar to that (1.5±0.8 kJ mol^{-1})[18] determined spectroscopically. The same model has been applied recently[14] to the series of cyclic ethers 2,5-dihydrofuran, oxetane and oxirane and their complexes with HF. Along this series, the internal ring angle COC decreases from 108° through ~90° to ~ 60°. The extended electric dipole moment model of HF suggested[14] that the angle 2ϕ between the n-pairs on O increases as the ring angle COC decreases.

We present here an investigation of the analogous series of thio-ethers, namely 2,5-dihydrothiophene, thietane and thiirane, in which the CSC ring angle also decreases from ~95° through ~77° to ~48°, respectively. Molecular diagrams of the three cyclic thioethers are set out in Figure 3. These were calculated at the CCSD(T)-F12c/cc-pVTZ-F12 level of theory, as described in Section 2. Given that the result described above for H_2S suggests an inter-n-pair angle of ~180°, the aim of the work described here is to determine how the inter-n-pair angle varies in the thioether series. The tools for the investigation are: (1) the electrostatic potential energy of a non-perturbing, unit positive around the S atom in each molecule, (2) the potential energy of the extended electric dipole moment model of HF around S, and (3) *ab initio* calculations of the geometries of the thioether$\cdots$HF complexes.

2. Computational details

The geometries of the interacting complexes and isolated molecules were optimised using the MOLPRO system[44,45] of *ab initio* programs with the explicitly correlated CCSD(T)-F12c method[46] [this is also sometimes referred to as CCSD(T)(F12*)].The triple-zeta correlation consistent basis sets for explicitly correlated methods, cc-pVTZ-F12, were used,[47] along with the cc-pVTZ-F12/MP2Fit,[48] cc-pVTZ/JKFit[49]

and cc-pVTZ-F12/OptRI[50] auxiliary basis sets. The geminal Slater exponent was 1.0 a_0^{-1}, and the geometries are provided as Supplementary Material.

The optimised geometries of the isolated molecules were then used in distributed multipole analyses (DMAs),[51] with detailed results of the latter available in the Supplementary Material. The first-order density matrix required for a DMA was calculated at the CCSD/cc-pV(5+d)Z level of theory,[52,53] where the +d denotes that the basis set includes additional "tight" d functions for sulfur.[54] Symmetry-adapted perturbation theory (SAPT)[55] calculations were carried out on some complexes in order to decompose the interaction energy into electrostatic, exchange, induction and dispersion components. The so-called "chemist's grouping" was used to assemble the individual SAPT2+(3)δMP2 components into the four above physical components.[56] All SAPT calculations were carried out with the Psi4 V1.2 program[57] using the aug-cc-pV(T+d)Z orbital basis set,[54,58,59] with density fitting enabled by the corresponding auxiliary basis sets.[60] Molecular electrostatic potential maps (MESPs) were generated at the MP2/6-311++G** level[61] by the SPARTAN package[62] with an iso-density surface of 0.001 e/bohr³.

3.   Results.

3.1   Electrostatic potential energy curves for 2,5-dihydrothiophene, thietane and thiirane

Figure 3 shows diagrams (drawn to scale) of the geometries of the three cyclic thioethers 2,5-dihydrothiophene, thietane and thiirane, as optimised at the CCSD(T)-F12c/cc-pVTZ-F12 level of theory. Details are available in the Supplementary Material. The ring atoms are co-planar in the equilibrium conformations of 2,5-dihydrothiophene and thietane, but the four membered ring is puckered in thietane, both conclusions in accord with those from rotational spectroscopy.[63–65] The angle of puckering of the ring in thietane (36°) is in agreement with that determined from the rotation-inversion spectrum.[65]

The electrostatic potential energy of a non-perturbing protonic charge $V(\phi)$ at a fixed distances $r = 2.169$ Å, 2.155 Å and 2.162 Å from the S atom as a function of the angle ϕ is shown in Figure 4 for thiirane, 2,5-dihydrothiophene and thietane, respectively. These are the equilibrium values from the CCSD(T)-F12c/cc-pVTZ-F12 calculations. The angle ϕ is that made by the vector r with the heavy-atom plane in 2,5-dihyrothiophene and thiirane and corresponds to the angle defined in Figures 1 and 2. For thietane, the plane in question is that made by S and its two contiguous C atoms.

The two equivalent minima in Figure 4 for thiirane and 2,5-dihydrothiophene occur at ± 80° and ±75°, respectively. The hydrogen-bonded complex thiirane···HF has been investigated in detail through its rotational spectrum,[66] the interpretation of which led to the angle $\phi = 86.5(11)°$, in reasonable agreement with the notion that HF lies along a n-pair direction, if the minima in Figure 4 correspond to n-pair

directions. According to Figure 4, the complex 2,5-dihydrothiophene⋯HF should have HF forming a hydrogen bond to S with an angle ϕ close to 80°, but this complex has yet to be investigated experimentally. Thietane has the four-membered ring puckered by 36° in the equilibrium geometry and therefore has C_s rather than C_{2v} symmetry. This means that the two n-pairs on S are no longer equivalent, a conclusion reflected in Figure 4, in which the $V(\phi)$ versus ϕ curve for thietane shows two inequivalent minima at approximately –70° and +65° but different in energy by only 9 kJ mol^{-1}. If these minima can be identified with the directions of n-pairs, we might refer to them as axial and equatorial n-pairs, respectively. In fact, Alonso and co-workers[67] have characterised two conformers of the complex thietane⋯HF in a supersonic expansion of the two component in helium, with angles $\phi_{axial} = -88.8(2)°$ and $\phi_{equat.} = 89.8(3)°$ and with the axial form having the greater population and therefore the low energy at the end of the expansion. The energy order of the minima in the $V(\phi)$ versus ϕ plot for thietane has the equatorial minimum lower in energy than that of the axial minimum and the ϕ_{min} values are somewhat smaller in magnitude than those from experiment. This is confirmed by a high-resolution, infrared spectroscopy investigation of thietane⋯HF.[68]

The conclusions from Figure 4 are broadly consistent with those that can be drawn from the molecular electrostatic surface potentials of the three cyclic thioethers, which are set out in Figure 5. The MESP in each case corresponds to an iso-density surface of 0.001 e/bohr^3 and was obtained by a SPARTAN calculation at the MP2/6-311++G** level of theory. Half the MESP has been cut away to reveal a tubular model of the molecule in each case. The MESPs of thiirane and 2,5-dihydrothiophene show two equivalent red spots above and below the S atom which make angles of $\phi \sim \pm 70\text{-}80°$ at S with the C_2 axis and correspond to the most nucleophilic regions of these molecules, presumably those along the n-pair axes. This reflects the two equivalent potential energy minima shown in Figure 4 for each of these molecules. On the other hand, the MESP for thietane shows clearly that the equatorial red spot (n-pair) is more nucleophilic than the axial n-pair for which, at the colour resolution employed, no red spot is evident. This observation is consistent with the result for the thietane $V(\phi)$ versus ϕ potential curve (Figure 4) which reveals that the equatorial position has the lowest electrostatic potential energy. The angle ϕ made by the equatorial red spot appears to be smaller than the corresponding angles in thiirane and 2,5-dihydrothiophene, in agreement with the conclusion from Figure 4.

3.2   Potential energy of an extended electric dipole moment model for HF interacting with 2,5-dihydrothiophene, thietane and thiirane

It was suggested some years ago that the geometry of a hydrogen-bonded complex B⋯HX, where B is a Lewis base and X is a halogen atom or a pseudo-halogen group, can be predicted by assuming that in the

equilibrium geometry the HX molecule lies along the axis of a n-pair carried by the acceptor atom of B.[12,13] As a corollary to this rule, it was suggested that, *e.g.* HF might act as a probe of n-pair directions. Persevering with electrostatics, a slightly more sophisticated approach to probing n-pair directions via electrostatic potential energy consists of using a non-perturbing extended electric dipole moment model for hydrogen fluoride in place of merely a non-perturbing, single protonic charge. Guided by the DMA for HF given in ref. 41, we choose a model of HF that consists of two charges $+0.540|e|$ and $-0.540|e|$ on H and F, respectively, separated by 0.9256 Å (the r_0 bond length of HF calculated from the rotational constant B_0).[69] This model ignores small electric dipoles and quadrupoles centred on H and F in ref. 41 and therefore corresponds to the zeroth-order approximation to the charge distribution of hydrogen fluoride as represented by its DMA. HF is assumed to lie on the line that subtends an angle ϕ at the S atom of the cyclic thioether, as defined earlier when evaluating electrostatic potential energy. Then, with the H atom of HF at an appropriate distance from S, the electrostatic potential energy of both charges is evaluated with the aid of the DMA of the cyclic ether and summed. The results of the energy $V_{HF}(\phi)$ as a function of ϕ are given in Figure 6. The S···H distances were 2.169 Å, 2.155 Å and 2.162 Å as previously used for the calculation of the electrostatic potential.

The angles ϕ at the minima in Figure 6 are $\pm 85.4(10)°$ for thiirane and $\pm 80.4(10)°$ for 2,5-dihydrothiophene. The two inequivalent minima for thietane are now at $\phi = 68.1(10)°$ and $79.5(10)°$ for the equatorial and axial positions, respectively, with the equatorial minimum again the lower in energy, but by only about 1.7 kJ mol^{-1}. It is worth noting that the angles ϕ when the extended electric dipole model for HF is used are larger and in somewhat better agreement with those of the MESPs in Figure 5 and with the experimental geometries of thiirane···HF[66] and thietane···HF[67] than when the simple electrostatic potential energy is used in the comparison. The angle ϕ at the equatorial position is again smaller than that at the axial position. A feature of Figure 6 is the rapid drop of the potential energy of HF around thietane at the angle $\phi \simeq +100°$ and greater. This arises because, when HF goes beyond the axial minimum, the nucleophilic F atom gets close to an electrophilic H atom [blue region in Figure 5(c) on C(2)]. A secondary attractive interaction of F and H-C(2) then becomes significant and causes the noted drop in energy. A secondary interaction is clearly present in the results from *ab initio* calculations to be discussed in Section 3.3 and shown in Figure 7 (c), but it is then moderated by the presence of exchange repulsion, which is absent from the extended electric dipole model of HF. Indeed, SAPT calculations on the two thietane···HF conformers show that a full *ab initio* treatment of the interaction energy places the axial conformer slightly lower in energy, with an electrostatic contribution of -48.57 kJ mol^{-1}, compared to -44.51 kJ mol^{-1} for the equatorial conformer.

3.3   Geometries of cyclic thioether···HF complexes from ab initio calculations

The equilibrium geometries of thiirane···HF, thietane···HF and 2,5-dihydrothiophene···HF calculated at the CCSD(T)-F12c/cc-pVTZ-F12 level of theory are represented as the scale models of the complexes shown in Figure 7. The values of the angle ϕ made by the red-dotted line from H to S (the hydrogen bond) with the C_2 axis in each of thiirane and 2,5-dihydrothiophene or with the local C_2 axis of the CSC fragment of thietane are indicated and given in the caption, together with the angle θ, which measures the angular deviation of the S···H–F nuclei from collinearity. Two low-energy conformers of thietane···HF were detected, namely the axial conformer having $\phi = 88.5°$ in Figure 7(c) and the equatorial conformer having $\phi = 76.6°$, with the former the lower in energy by 1.41 kJ mol^{-1}. This is the energy order deduced by Alonso and co-workers[67] from their analysis of the rotational spectra of the two forms. These authors report r_0 values of 88.8(2)° and 89.8(3)° for the axial and equatorial conformers, respectively. The equilibrium values of ϕ for the two conformers (see caption to Figure 7) are both larger by about 8-9° than those [79.5(1)° and 68.1(10)°] obtained by using the extended electric dipole model of HF in Section 3.2. The ϕ_e values for thiirane and 2,5-dihydrothiophene (93.1° and $\phi = 84.5°$, respectively) are likewise larger by about 7° and 4° than those [85.4(10)° and 80.4(10)°, respectively] from the extended electric dipole model of HF. A possible reason for this under-estimation of the angles ϕ by the model can be identified by considering the angular non-linearities θ.

All geometries shown in Figure 7 exhibit non-linear hydrogen bonds formed by HF to a n-pair on S. The angular non-linearities θ clearly arise from secondary interactions of F (the nucleophilic end of HF) with the regions near H atoms of the cyclic thioether. In a thought experiment, we might envisage that the HF molecule is initially constrained to approach along an axis of a n-pair on S and then the secondary interaction is switched on. The F atom moves towards an electrophilic H atom, the movement largely pivoted at H of HF but presumably there is some movement of the H (of HF) in the same direction. The larger the secondary interaction, the greater the movement of H and the greater the non-linearity. Thus, as well as causing the hydrogen bond to be non-linear, this model leads ϕ to increase from that defined by the n-pair direction. In this context, we note that the angles ϕ and the non-linearities θ are $\phi = 93.1°$ and $\theta = 21.1°$ for thiirane···HF, $\phi = 84.5°$ and $\theta = 10.3°$ for 2,5-dihydrothiophene···HF, (c) $\phi = 88.5°$ and $\theta = 14.1°$ for *axial*-thietane···HF. Larger deviations of θ from zero tend to be associated with larger positive deviations $\Delta\phi$ of ϕ from the n-pair angle, which (according to the extended electric dipole model of HF as a probe) is in the range 80-85° for these three cases. The values of the ($\Delta\phi$, θ) pairs are (7.6°, 21.1°), (9.0°,14.1°) and (4.1°, 10.3°) for thiirane···HF, *axial*-thietane···HF and 2,5-dihydrothiophene···HF, respectively. For *equatorial*-thietane···HF, the same model gives the angle $\phi = 68.1°$ for the other n-pair of S, which, because the *ab initio* value is $\phi = 76.6°$, implies that a positive deviation $\Delta\phi = 8.5°$ accompanies the non-linearity $\theta = 17.5°$ for this conformer. The values of θ have been measured experimentally to be 16.8(13)°, 8(4)°, and 12(6)° for the first three members of the series.[66,67]

4. Conclusions.

To probe the nucleophilic regions of cyclic thioethers in connection with predicting geometries of intermolecular complexes, the electrostatic potential energy $V(\phi)$ of a non-perturbing, protonic charge at a fixed distance r from the S atom in three cyclic thioethers has been examined as a function of the angle ϕ made by the $\boldsymbol{r}$-vector with the C_2 axis (in thiirane and 2,5-dihydrothiophene) or the local C_2 axis associated with the C–S–C moiety of the thietane puckered ring. The results have been compared with molecular electrostatic surface potentials of the three cyclic thioethers. The electrostatic potential energy $V_{HF}(\phi)$ of HF modelled as an extended electric dipole has also been calculated as a function of the angle ϕ. Finally, the geometries of the complexes thiirane···HF, thietane···HF and 2,5-dihydrothiophene···HF were optimised at the CCSD(T)-F12c/cc-pVTZ-F12 level of theory. The positions of the minima in the $V_{HF}(\phi)$ versus ϕ functions are in good agreement with the directions of maximum nucleophilicity exhibited in the MESP diagrams of the cyclic thioethers. In the simplest electrostatic model, the minima $|\phi_{\min}|$ in the $V(\phi)$ versus ϕ functions occur at smaller values, the reason for which has been discussed elsewhere.[14] In the thioether···HF complexes, the *ab initio* calculations reveal that atoms S···H–F deviate from collinearity by an angle θ in a direction that suggests a secondary interaction of the nucleophilic region of F with electrophilic H atoms attached to ring carbon atoms. The *ab initio* calculations also find that the angles ϕ made by the S···H hydrogen bond with the C_2 (or local C_2) axes are systematically larger than those at the minima in the $V_{HF}(\phi)$ versus ϕ functions. This systematic difference can be explained by using a simple model of complex formation that accounts for secondary interactions between the nucleophilic F and regions near hydrogen atoms of the cyclic thioether.

If it can be assumed that the minima of the $V_{HF}(\phi)$ versus ϕ potential energy function (resulting from the model in which HF is treated as an extended electric dipole) provide a method of locating non-bonding electron pairs, there is no evidence that the half-angle between the n-pairs on S increases along the series 2,5-dihydrothiophene, *axial*-thietane, thiirane as the ring angle CSC decreases from 94.9° through 76.7° to 47.9°. Indeed, the values of $\phi_{\min}$ are 80.4(10)°, 79.5(10)° and 85.4(10)°, respectively, so that 2,5-dihydrothiophene has the largest ring angle but an inter-n-pair angle that is insignificantly different from that of *axial*-thietane. There is evidence of a small increase when the ring angle is very small in thiirane. (The *equatorial* n-pair of thietane has been excluded from this discussion because of the distorting effect that the secondary interaction mentioned in Section 3.2 has on the potential curve when unmoderated by exchange repulsion). In the corresponding series in which the ring heteroatom is oxygen, namely 2,5-dihydrofuran, oxetane and oxirane, and in which a similar decrease of ring angle obtains, there is evidence of a significant increase in the inter-n-pair angle as the ring angle decreases.[14] Presumably, if the n-pairs on S are in two sp hybrids and the CS bonds involve two orthogonal p orbitals on S, there is only small scope for changing the hybridisation at S as the ring angle deceases. Accordingly, the inter-n-pair angle changes

only slightly in the series of cyclic thioethers. This explanation implies increasingly bent S–C bonds as the ring angle at S decreases.

5   Acknowledgements

6   References

(1)   Arunan, E.; Desiraju, G. R.; Klein, R. A.; Sadlej, J.; Scheiner, S.; Alkorta, I.; Clary, D. C.; Crabtree, R. H.; Dannenberg, J. J.; Hobza, P.; et al. Definition of the Hydrogen Bond (IUPAC Recommendations 2011). *Pure Appl. Chem.* **2011**, *83* (8), 1637–1641. https://doi.org/10.1351/PAC-REC-10-01-02.
(2)   Desiraju, G. R.; Ho, P. S.; Kloo, L.; Legon, A. C.; Marquardt, R.; Metrangolo, P.; Politzer, P.; Resnati, G.; Rissanen, K. Definition of the Halogen Bond (IUPAC Recommendations 2013). *Pure Appl. Chem.* **2013**, *85* (8), 1711–1713. https://doi.org/10.1351/PAC-REC-12-05-10.
(3)   Clark, T.; Hennemann, M.; Murray, J. S.; Politzer, P. Halogen Bonding: The σ-Hole: Proceedings of "Modeling Interactions in Biomolecules II", Prague, September 5th–9th, 2005. *J. Mol. Model.* **2007**, *13* (2), 291–296. https://doi.org/10.1007/s00894-006-0130-2.
(4)   Murray, J. S.; Lane, P.; Clark, T.; Riley, K. E.; Politzer, P. σ-Holes, π-Holes and Electrostatically-Driven Interactions. *J. Mol. Model.* **2012**, *18* (2), 541–548. https://doi.org/10.1007/s00894-011-1089-1.
(5)   Clark, T.; Politzer, P.; Murray, J. S. Correct Electrostatic Treatment of Noncovalent Interactions: The Importance of Polarization. *Wiley Interdiscip. Rev. Comput. Mol. Sci.* **2015**, *5* (2), 169–177. https://doi.org/10.1002/wcms.1210.
(6)   Wang, C.; Guan, L.; Danovich, D.; Shaik, S.; Mo, Y. The Origins of the Directionality of Noncovalent Intermolecular Interactions. *J. Comput. Chem.* **2016**, *37* (1), 34–45. https://doi.org/10.1002/jcc.23946.
(7)   Mustoe, C. L.; Gunabalasingam, M.; Yu, D.; Patrick, B. O.; Kennepohl, P. Probing Covalency in Halogen Bonds through Donor K-Edge X-Ray Absorption Spectroscopy: Polyhalides as Coordination Complexes. *Faraday Discuss.* **2017**, *203*, 79–91. https://doi.org/10.1039/C7FD00076F.
(8)   Scheiner, S. The Interplay between Charge Transfer, Rehybridization, and Atomic Charges in the Internal Geometry of Subunits in Noncovalent Interactions. *Int. J. Quantum Chem.* **2015**, *115* (1), 28–33. https://doi.org/10.1002/qua.24789.
(9)   Kolář, M. H.; Hobza, P. Computer Modeling of Halogen Bonds and Other σ-Hole Interactions. *Chem. Rev.* **2016**, *116* (9), 5155–5187. https://doi.org/10.1021/acs.chemrev.5b00560.
(10)   Stone, A. J. Are Halogen Bonded Structures Electrostatically Driven? *J. Am. Chem. Soc.* **2013**, *135* (18), 7005–7009. https://doi.org/10.1021/ja401420w.
(11)   Hill, J. G.; Legon, A. C. On the Directionality and Non-Linearity of Halogen and Hydrogen Bonds. *Phys. Chem. Chem. Phys.* **2015**, *17* (2), 858–867. https://doi.org/10.1039/C4CP03376K.
(12)   Legon, A. C.; Millen, D. J. Determination of Properties of Hydrogen-Bonded Dimers by Rotational Spectroscopy and a Classfication of Dimer Geometries. *Faraday Discuss. Chem. Soc.* **1982**, *73*, 71. https://doi.org/10.1039/dc9827300071.
(13)   Legon, A. C.; Millen, D. J. Angular Geometries and Other Properties of Hydrogen-Bonded Dimers: A Simple Electrostatic Interpretation of the Success of the Electron-Pair Model. *Chem. Soc. Rev.* **1987**, *16*, 467. https://doi.org/10.1039/cs9871600467.

(14)   Hill, J. G.; Legon, A. C. Electrostatic Potential and a Simple Extended Electric Dipole Model of Hydrogen Fluoride as Probes of Non-Bonding Electron Pairs in the Cyclic Ethers 2,5-Dihydrofuran, Oxetane and Oxirane. *Crystals* **2017**, *7* (9), 261. https://doi.org/10.3390/cryst7090261.

(15)   Shields, Z. P.; Murray, J. S.; Politzer, P. Directional Tendencies of Halogen and Hydrogen Bonds. *Int. J. Quantum Chem.* **2010**, *110* (15), 2823–2832. https://doi.org/10.1002/qua.22787.

(16)   Bevan, J. W.; Legon, A. C.; Millen, D. J.; Rogers, S. C. Existence and Molecular Properties of a Gas-Phase, Hydrogen-Bonded Complex between Hydrogen Fluoride and Water Established from Microwave Spectroscopy. *J. Chem. Soc. Chem. Commun.* **1975**, No. 9, 341. https://doi.org/10.1039/c39750000341.

(17)   Bevan, J. W.; Kisiel, Z.; Legon, A. C.; Millen, D. J.; Rogers, S. C. Spectroscopic Investigations of Hydrogen Bonding Interactions in the Gas Phase. IV. The Heterodimer $H_2O\cdots HF$: The Observation and Analysis of Its Microwave Rotational Spectrum and the Determination of Its Molecular Geometry and Electric Dipole Moment. *Proc. R. Soc. Math. Phys. Eng. Sci.* **1980**, *372* (1750), 441–451. https://doi.org/10.1098/rspa.1980.0121.

(18)   Kisiel, Z.; Legon, A. C.; Millen, D. J. Spectroscopic Investigations of Hydrogen Bonding Interactions in the Gas Phase. VII. The Equilibrium Conformation and Out-of-Plane Bending Potential Energy Function of the Hydrogen-Bonded Heterodimer $H_2O\cdots HF$ Determined from Its Microwave Rotational Spectrum. *Proc. R. Soc. Math. Phys. Eng. Sci.* **1982**, *381* (1781), 419–442. https://doi.org/10.1098/rspa.1982.0081.

(19)   Legon, A. C.; Willoughby, L. C. Identification and Molecular Geometry of a Weakly Bound Dimer (H_2O, HCl) in the Gas Phase by Rotational Spectroscopy. *Chem. Phys. Lett.* **1983**, *95* (4–5), 449–452. https://doi.org/10.1016/0009-2614(83)80592-2.

(20)   Kisiel, Z.; Pietrewicz, B. A.; Fowler, P. W.; Legon, A. C.; Steiner, E. Rotational Spectra of the Less Common Isotopomers, Electric Dipole Moment and the Double Minimum Inversion Potential of $H_2O\cdots HCl$. *J. Phys. Chem. A* **2000**, *104* (30), 6970–6978. https://doi.org/10.1021/jp001156o.

(21)   Legon, A. C.; Suckley, A. P. Br Nuclear Quadrupole and H,Br Nuclear-Spin-Nuclear-Spin Coupling in the Rotational Spectrum of $H_2O\cdots HBr$. *Chem. Phys. Lett.* **1988**, *150* (1–2), 153–158. https://doi.org/10.1016/0009-2614(88)80413-5.

(22)   McIntosh, A.; Walther, T.; Lucchese, R. R.; Bevan, J. W.; Suenram, R. D.; Legon, A. C. The Microwave Spectrum and Ground-State Structure of $H_2O\cdots HI$. *Chem. Phys. Lett.* **1999**, *314* (1–2), 57–64. https://doi.org/10.1016/S0009-2614(99)01027-1.

(23)   Viswanathan, R.; Dyke, T. R. The Structure of $H_2S\cdot HF$ and the Stereochemistry of the Hydrogen Bond. *J. Chem. Phys.* **1982**, *77* (3), 1166–1174. https://doi.org/10.1063/1.443981.

(24)   Willoughby, L. C.; Fillery-Travis, A. J.; Legon, A. C. An Investigation of the Rotational Spectrum of $H_2S\cdots HF$ by Pulsed-nozzle, Fourier-transform Microwave Spectroscopy: Determination of the Hyperfine Coupling Constants χ_{Aa} (^{33}S), χ^D_{Aa}, and $D^{H(D)F}_{Aa}$. *J. Chem. Phys.* **1984**, *81* (1), 20–26. https://doi.org/10.1063/1.447364.

(25)   Goodwin, E. J.; Legon, A. C. Microwave Rotational Spectrum of a Weakly Bound Complex Formed by Hydrogen Sulphide and Hydrogen Chloride. *J. Chem. Soc. Faraday Trans. 2* **1984**, *80* (1), 51. https://doi.org/10.1039/f29848000051.

(26)   Jaman, A. I.; Legon, A. C. Rotational Spectrum of the Hydrogen-Bonded Heterodimer $H_2S\cdots HBr$. *J. Mol. Struct.* **1986**, *145* (3–4), 261–276. https://doi.org/10.1016/0022-2860(86)85030-X.

(27)   Suckley, A. P. PhD thesis, University of London, 1991.

(28)   Cooke, S. A.; Cotti, G.; Evans, C. M.; Holloway, J. H.; Legon, A. C. Rotational Spectrum and Properties of a Gas-Phase Complex of Molecular Fluorine and Hydrogen Cyanide. *Chem. Phys. Lett.* **1996**, *262* (3–4), 308–314. https://doi.org/10.1016/0009-2614(96)01065-2.

(29)   Cooke, S. A.; Cotti, G.; Evans, C. M.; Holloway, J. H.; Legon, A. C. The Pre-Reactive Complex $H_2O\cdots ClF$ Identified in Mixtures of Water Vapour and Chlorine Monofluoride by Rotational Spectroscopy. *Chem Commun* **1996**, No. 20, 2327–2328. https://doi.org/10.1039/CC9960002327.

(30)   Cooke, S. A.; Cotti, G.; Evans, C. M.; Holloway, J. H.; Kisiel, Z.; Legon, A. C.; Thumwood, J. M. A. Pre-Reactive Complexes in Mixtures of Water Vapour with Halogens: Characterisation of

H$_2$O···ClF and H$_2$O···F$_2$ by a Combination of Rotational Spectroscopy and Ab Initio Calculations. *Chem. - Eur. J.* **2001**, *7* (11), 2295–2305. https://doi.org/10.1002/1521-3765(20010601)7:11<2295::AID-CHEM22950>3.0.CO;2-T.

(31)   Davey, J. B.; Legon, A. C.; Waclawik, E. R. An Investigation of the Gas-Phase Complex of Water and Iodine Monochloride by Microwave Spectroscopy: Geometry, Binding Strength and Electron Redistribution. *Phys. Chem. Chem. Phys.* **2000**, *2* (8), 1659–1665. https://doi.org/10.1039/b000526f.

(32)   Davey, J. B.; Legon, A. C.; Thumwood, J. M. A. Interaction of Water and Dichlorine in the Gas Phase: An Investigation of H$_2$O···Cl$_2$ by Rotational Spectroscopy and Ab Initio Calculations. *J. Chem. Phys.* **2001**, *114* (14), 6190–6202. https://doi.org/10.1063/1.1354178.

(33)   Davey, J. B.; Legon, A. C. Rotational Spectroscopy of the Gas Phase Complex of Water and Bromine Monochloride in the Microwave Region: Geometry, Binding Strength and Charge Transfer. *Phys. Chem. Chem. Phys.* **2001**, *3* (15), 3006–3011. https://doi.org/10.1039/b103351b.

(34)   Legon, A. C.; Thumwood, J. M. A.; Waclawik, E. R. The Interaction of Water and Dibromine in the Gas Phase: An Investigation of the Complex H$_2$O···Br$_2$ by Rotational Spectroscopy and Ab Initio Calculations. *Chem. - Eur. J.* **2002**, *8* (4), 940–950. https://doi.org/10.1002/1521-3765(20020215)8:4<940::AID-CHEM940>3.0.CO;2-H.

(35)   Bloemink, H. I.; Dolling, S. J.; Hinds, K.; Legon, A. C. H$_2$S···Cl$_2$ Characterised in a Pre-Reactive Gas Mixture of Hydrogen Sulfide and Chlorine through Rotational Spectroscopy: The Nature of the Interaction. *J Chem Soc Faraday Trans* **1995**, *91* (14), 2059–2066. https://doi.org/10.1039/FT9959102059.

(36)   Bloemink, H. I.; Hinds, K.; Holloway, J. H.; Legon, A. C. Isolation of H$_2$S···ClF in a Pre-Reactive Mixture of H$_2$S and ClF Expanded in a Coaxial Jet and Characterisation by Rotational Spectroscopy. *Chem. Phys. Lett.* **1995**, *242* (1–2), 113–120. https://doi.org/10.1016/0009-2614(95)00694-Y.

(37)   Bloemink, H. I.; Legon, A. C. The Pre-Reactive Complex of H$_2$S and BrCl; Observation and Characterisation by Rotational Spectroscopy. *Chem. - Eur. J.* **1996**, *2* (3), 265–270. https://doi.org/10.1002/chem.19960020306.

(38)   Cooke, S. A.; Cotti, G.; Holloway, J. H.; Legon, A. C. Detection and Characterization of a Pre-Reactive Complex in a Mixture of Water and Fluorine: Rotational Spectrum of H$_2$O···F$_2$. *Angew. Chem. Int. Ed. Engl.* **1997**, *36* (12), 129–130. https://doi.org/10.1002/anie.199701291.

(39)   Legon, A. C.; Waclawik, E. R. Angular Geometry, Binding Strength and Charge Transfer for the Complex H$_2$S···ICl Determined by Rotational Spectroscopy. *Chem. Phys. Lett.* **1999**, *312* (5–6), 385–393. https://doi.org/10.1016/S0009-2614(99)00983-5.

(40)   Legon, A. C.; Thumwood, J. M. A. Properties of the Halogen-Bonded Complex H$_2$S···Br$_2$ Established by Rotational Spectroscopy and Ab Initio Calculations. *Phys. Chem. Chem. Phys.* **2001**, *3* (14), 2758–2764. https://doi.org/10.1039/b102540f.

(41)   Buckingham, A. D.; Fowler, P. W. A Model for the Geometries of Van Der Waals Complexes. *Can. J. Chem.* **1985**, *63* (7), 2018–2025. https://doi.org/10.1139/v85-334.

(42)   Johnson, E. R.; Keinan, S.; Mori-Sánchez, P.; Contreras-García, J.; Cohen, A. J.; Yang, W. Revealing Noncovalent Interactions. *J. Am. Chem. Soc.* **2010**, *132* (18), 6498–6506. https://doi.org/10.1021/ja100936w.

(43)   Contreras-García, J.; Johnson, E. R.; Keinan, S.; Chaudret, R.; Piquemal, J.-P.; Beratan, D. N.; Yang, W. NCIPLOT: A Program for Plotting Noncovalent Interaction Regions. *J. Chem. Theory Comput.* **2011**, *7* (3), 625–632. https://doi.org/10.1021/ct100641a.

(44)   Werner, H.-J.; Knowles, P. J.; Knizia, G.; Manby, F. R.; Schütz, M.; Celani, P.; Györffy, W.; Kats, D.; Korona, T.; Lindh, R.; et al. *MOLPRO 2015.1*; see www.molpro.net, 2015.

(45)   Werner, H.-J.; Knowles, P. J.; Knizia, G.; Manby, F. R.; Schütz, M. Molpro: A General-Purpose Quantum Chemistry Program Package. *Wiley Interdiscip. Rev. Comput. Mol. Sci.* **2012**, *2* (2), 242–253. https://doi.org/10.1002/wcms.82.

(46) Hättig, C.; Tew, D. P.; Köhn, A. Communications: Accurate and Efficient Approximations to Explicitly Correlated Coupled-Cluster Singles and Doubles, CCSD-F12. *J. Chem. Phys.* **2010**, *132* (23), 231102. https://doi.org/10.1063/1.3442368.

(47) Peterson, K. A.; Adler, T. B.; Werner, H.-J. Systematically Convergent Basis Sets for Explicitly Correlated Wavefunctions: The Atoms H, He, B–Ne, and Al–Ar. *J. Chem. Phys.* **2008**, *128* (8), 084102. https://doi.org/10.1063/1.2831537.

(48) Kritikou, S.; Hill, J. G. Auxiliary Basis Sets for Density Fitting in Explicitly Correlated Calculations: The Atoms H–Ar. *J. Chem. Theory Comput.* **2015**, *11* (11), 5269–5276. https://doi.org/10.1021/acs.jctc.5b00816.

(49) Weigend, F. A Fully Direct RI-HF Algorithm: Implementation, Optimised Auxiliary Basis Sets, Demonstration of Accuracy and Efficiency. *Phys. Chem. Chem. Phys.* **2002**, *4* (18), 4285–4291. https://doi.org/10.1039/b204199p.

(50) Yousaf, K. E.; Peterson, K. A. Optimized Auxiliary Basis Sets for Explicitly Correlated Methods. *J. Chem. Phys.* **2008**, *129* (18), 184108. https://doi.org/10.1063/1.3009271.

(51) Stone, A. J. Distributed Multipole Analysis, or How to Describe a Molecular Charge Distribution. *Chem. Phys. Lett.* **1981**, *83* (2), 233–239. https://doi.org/10.1016/0009-2614(81)85452-8.

(52) Korona, T.; Moszynski, R.; Jeziorski, B. Electrostatic Interactions between Molecules from Relaxed One-Electron Density Matrices of the Coupled Cluster Singles and Doubles Model. *Mol. Phys.* **2002**, *100* (11), 1723–1734. https://doi.org/10.1080/00268970110105424.

(53) Dunning, Jr., T. H. Gaussian Basis Sets for Use in Correlated Molecular Calculations. I. The Atoms Boron through Neon and Hydrogen. *J. Chem. Phys.* **1989**, *90*, 1007–1023.

(54) Dunning, T. H.; Peterson, K. A.; Wilson, A. K. Gaussian Basis Sets for Use in Correlated Molecular Calculations. X. The Atoms Aluminum through Argon Revisited. *J. Chem. Phys.* **2001**, *114* (21), 9244–9253. https://doi.org/10.1063/1.1367373.

(55) Jeziorski, B.; Moszynski, R.; Szalewicz, K. Perturbation Theory Approach to Intermolecular Potential Energy Surfaces of van Der Waals Complexes. *Chem. Rev.* **1994**, *94* (7), 1887–1930. https://doi.org/10.1021/cr00031a008.

(56) Hohenstein, E. G.; Sherrill, C. D. Wavefunction Methods for Noncovalent Interactions: Noncovalent Interactions. *Wiley Interdiscip. Rev. Comput. Mol. Sci.* **2012**, *2* (2), 304–326. https://doi.org/10.1002/wcms.84.

(57) Parrish, R. M.; Burns, L. A.; Smith, D. G. A.; Simmonett, A. C.; DePrince, A. E.; Hohenstein, E. G.; Bozkaya, U.; Sokolov, A. Y.; Di Remigio, R.; Richard, R. M.; et al. Psi4 1.1: An Open-Source Electronic Structure Program Emphasizing Automation, Advanced Libraries, and Interoperability. *J. Chem. Theory Comput.* **2017**, *13* (7), 3185–3197. https://doi.org/10.1021/acs.jctc.7b00174.

(58) Kendall, R. A.; Dunning, Jr., T. H.; Harrison, R. J. Electron Affinities of the First-row Atoms Revisited. Systematic Basis Sets and Wave Functions. *J. Chem. Phys.* **1992**, *96* (9), 6796–6806. https://doi.org/10.1063/1.462569.

(59) Woon, D. E.; Dunning, T. H. Gaussian Basis Sets for Use in Correlated Molecular Calculations. III. The Atoms Aluminum through Argon. *J. Chem. Phys.* **1993**, *98* (2), 1358–1371. https://doi.org/10.1063/1.464303.

(60) Hohenstein, E. G.; Sherrill, C. D. Density Fitting of Intramonomer Correlation Effects in Symmetry-Adapted Perturbation Theory. *J. Chem. Phys.* **2010**, *133* (1), 014101. https://doi.org/10.1063/1.3451077.

(61) Krishnan, R.; Binkley, J. S.; Seeger, R.; Pople, J. A. Self-consistent Molecular Orbital Methods. XX. A Basis Set for Correlated Wave Functions. *J. Chem. Phys.* **1980**, *72* (1), 650–654. https://doi.org/10.1063/1.438955.

(62) *SPARTAN 14*; Wavefunction, Inc.: Irvine, USA, 2014.

(63) Durig, J. R.; Li, Y. S.; Durig, D. T. Spectra and Structure of Small Ring Compounds. XLII. Microwave Spectrum of 2,5-dihydrothiophene. *J. Chem. Phys.* **1981**, *74* (3), 1564–1567. https://doi.org/10.1063/1.441297.

(64) Hirao, T.; Okabayashi, T.; Tanimoto, M. The r_0 Structure of Ethylene Sulfide. *J. Mol. Spectrosc.* **2001**, *208* (1), 148–149. https://doi.org/10.1006/jmsp.2001.8362.

(65) Harris, D. O.; Harrington, H. W.; Luntz, A. C.; Gwinn, W. D. Microwave Spectrum, Vibration—Rotation Interaction, and Potential Function for the Ring-Puckering Vibration of Trimethylene Sulfide. *J. Chem. Phys.* **1966**, *44* (9), 3467–3480. https://doi.org/10.1063/1.1727251.

(66) Atkins, M. J.; Legon, A. C.; Warner, H. E. The Angular Geometry of Thiirane ⋯ HF and the Nonlinearity of the Hydrogen Bond from Rotational Spectroscopy. *Chem. Phys. Lett.* **1994**, *229* (3), 267–272. https://doi.org/10.1016/0009-2614(94)01049-8.

(67) Sanz, M. E.; López, J. C.; Alonso, J. L. Axial and Equatorial Hydrogen-Bond Conformers and Ring-Puckering Motion in the Trimethylene Sulfide·Hydrogen Fluoride Complex. *Chem. - Eur. J.* **2002**, *8* (18), 4265–4271. https://doi.org/10.1002/1521-3765(20020916)8:18<4265::AID-CHEM4265>3.0.CO;2-4.

(68) Madebène, B.; Asselin, P.; Soulard, P.; Alikhani, M. E. Axial and Equatorial Hydrogen-Bond Conformers between $(CH_2)_3S$ and H(D)F: Fourier Transform Infrared Spectroscopy and Ab Initio Calculations. *Phys. Chem. Chem. Phys.* **2011**, *13* (31), 14202. https://doi.org/10.1039/c1cp20668k.

(69) Guelachvili, G. Absolute Wavenumber Measurements of 1-0, 2-0, HF and 2-0, $H^{35}Cl$, $H^{37}Cl$ Absorption Bands. *Opt. Commun.* **1976**, *19* (1), 150–154. https://doi.org/10.1016/0030-4018(76)90408-9.
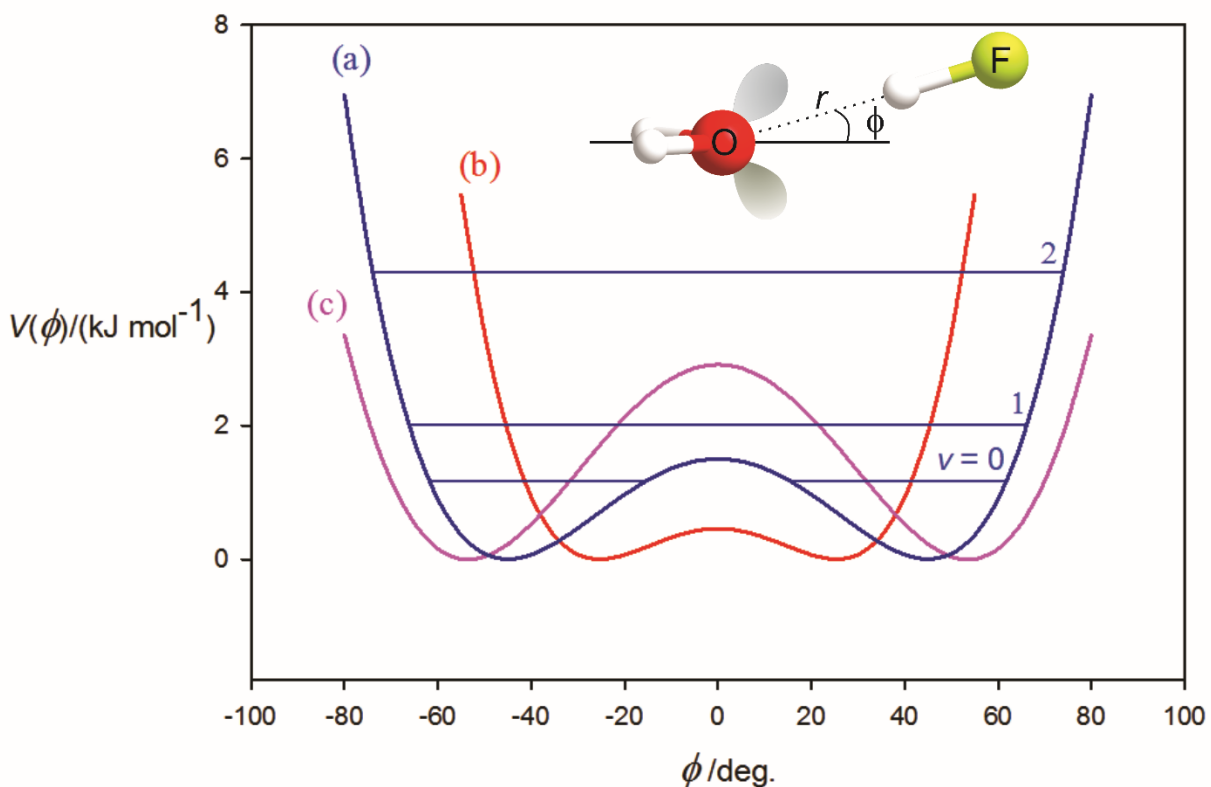
Figure 1. Curve (a) is the experimentally determined potential energy function associated with the low-frequency bending mode of $H_2O\cdots HF$ (blue) and associated energy levels (see ref. 18) The configuration at O is rapidly inverting so that in the zero-point ($v=0$) state the vibrational wavefunction has C_{2v} symmetry and the molecule is effectively planar. At equilibrium the configuration is pyramidal at O. The red curve (b) is the electrostatic potential energy of a non-perturbing, protonic charge place at a distance of $r=1.74$ Å from O (the experimental $r(O\cdots H)$ distance in $H_2O\cdots HF$) calculated by using the DMA obtained from the CCSD/cc-pV5Z wavefunction to represent the H_2O charge distribution.. The pink curve (c) is the potential energy obtained by using the same charge distribution for H_2O, but with the extended electric dipole model for hydrogen fluoride (see text for discussion) at the experimental distance .
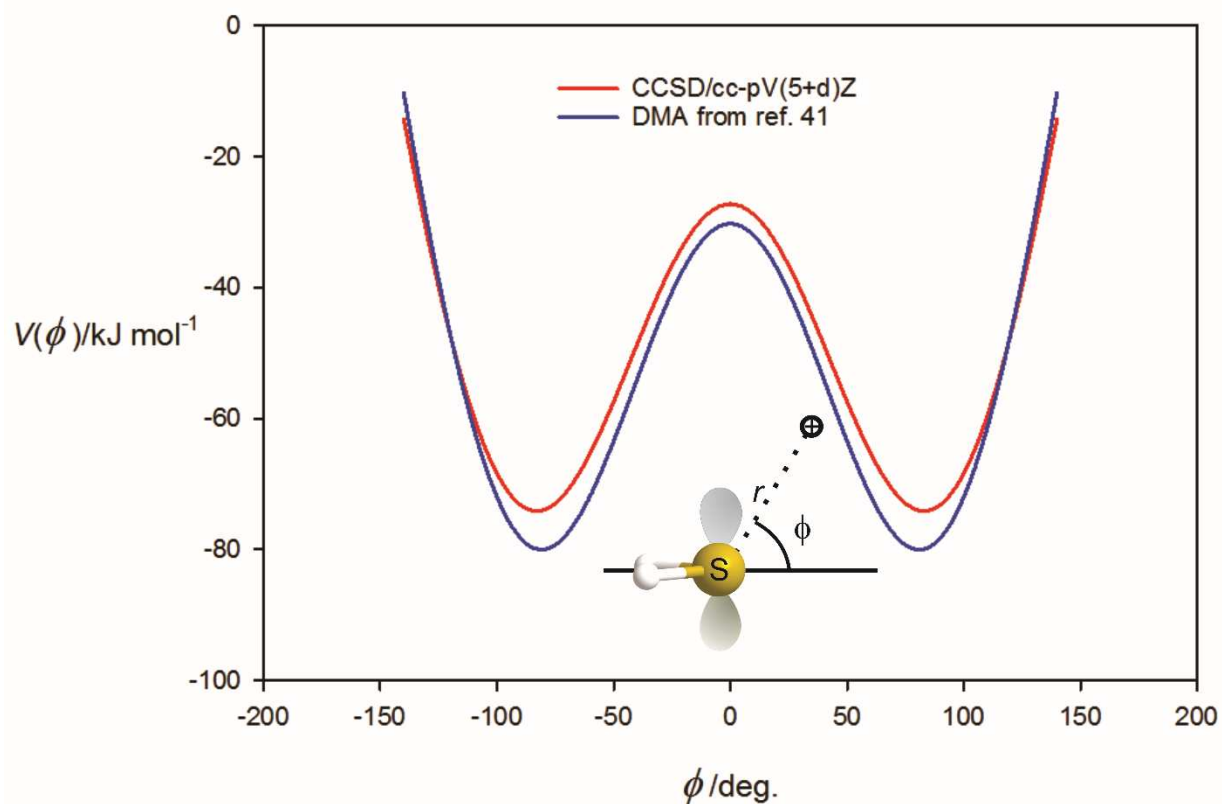
Figure 2. Electrostatic potential energy $V(\phi)$ of a non-perturbing, protonic charge in the plane perpendicular to plane of the H_2S nuclei as a function of the angle ϕ at a fixed distance $r = 2.31$ Å from S [the experimental distance $r(S\cdots H)$ in $H_2S\cdots HF$]. The blue (lower) curve results from use of the DMA given in ref. 41 to calculate $V(\phi)$. The red curve was generated by using the DMA of H_2S obtained from the CCSD/cc-pV(5+d)Z wavefunction.
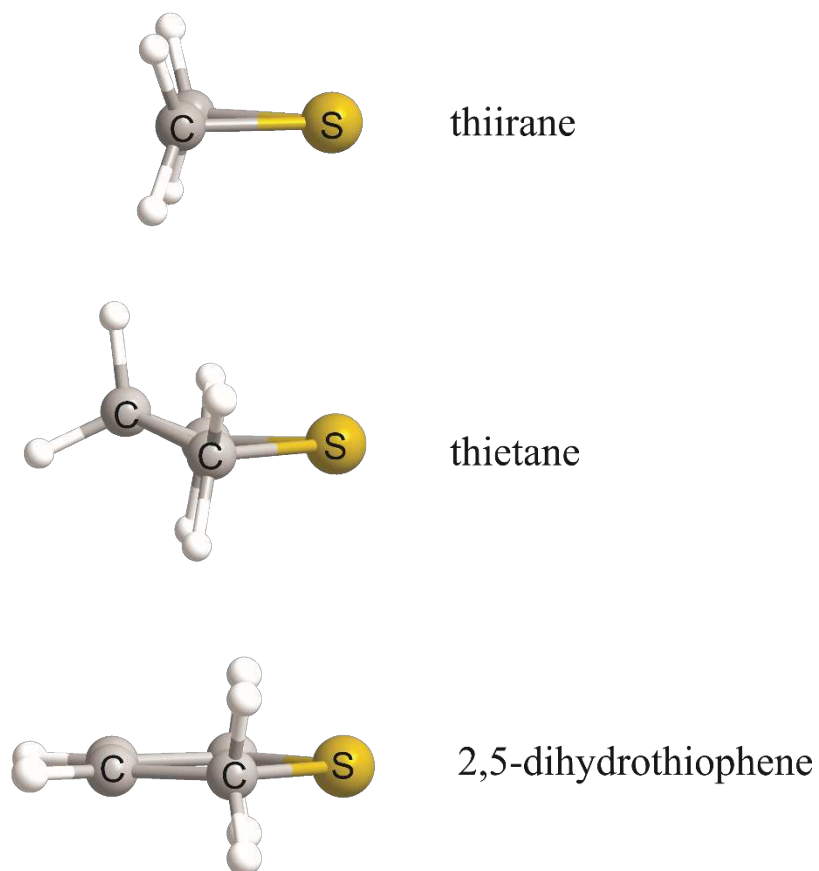
Figure 3. Models of the geometries of the three cyclic thioethers thiirane, thietane and 2,5-dihydrothiophene (to scale). The geometries are those that result from calculations at the CCSD(T)-F12c/cc-pVTZ-F12 level of theory.
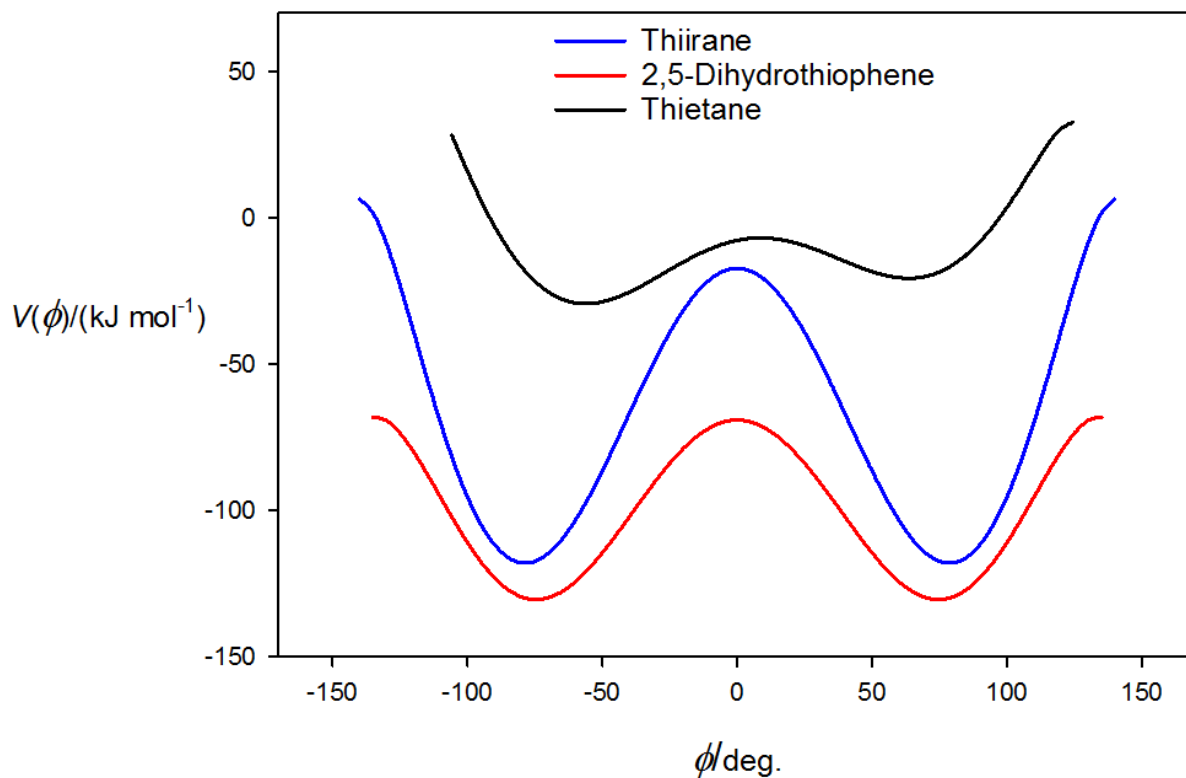
Figure 4. Electrostatic potential energy of a non-perturbing protonic charge at constant distances r = 2.169 Å, 2.162 Å and 2.155 Å from the S atom as a function of the angle ϕ in thiirane, thietane and 2,5-dihydrothiophene, respectively. In thiirane and 2,5-dihydrothiophene the angle ϕ is the angle made by the vector r with the plane of the ring atoms, as defined in Figure 1. In thietane, ϕ is the angle made by r with the plane defined by the S atom and its two contiguous C atoms. For clarity, 50 kJ mol^{-1} has been added to each point on the thietane curve.
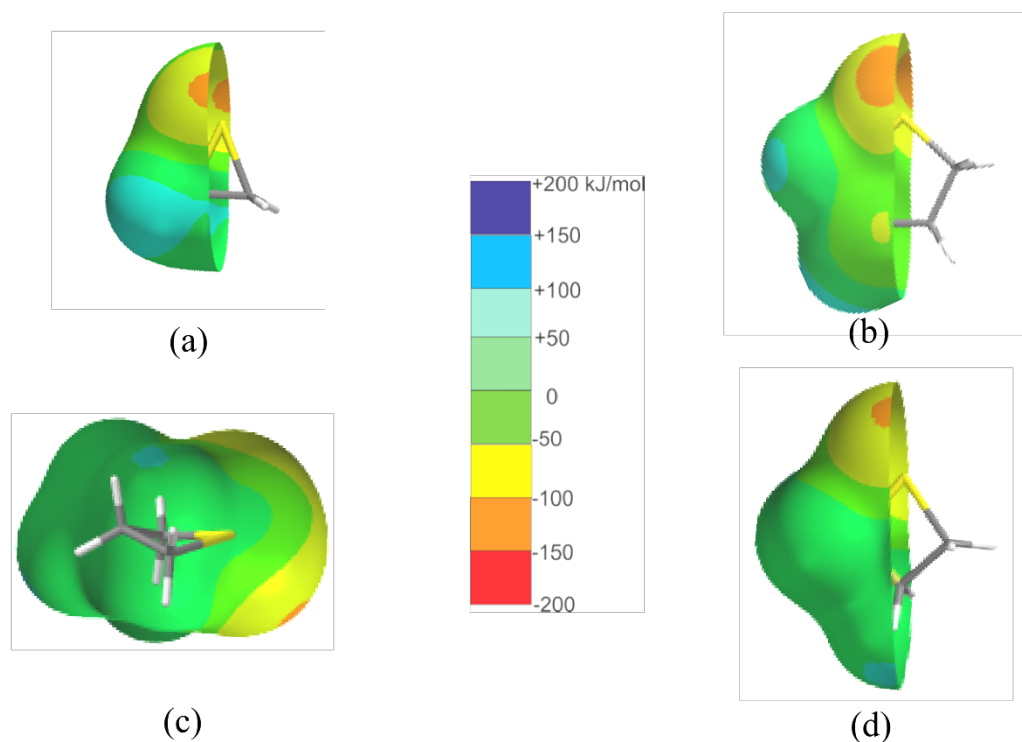
Figure 5. Molecular electrostatic surface potentials (MESPs) of (a) thiirane, (b) 2,5-dihydrothiophene, (c) and (d) thietane, calculated at iso-surfaces having a density of 0.001 e/bohr³. In each case, half of the MESP has been cut away to reveal a tubular model of the molecule within. The thiirane and 2,5-dihydrothiophene molecules have been rotated slightly about their C_2 axes anti-clockwise to show some of the inside of the MESP. The red spots on the upper and lower surfaces apparent in both thiirane and 2,5-dihydrothiophene represent the most nucleophilic regions of the molecules and may be identified with directions of the n-pairs on S. In (c), the thietane molecule is viewed from the side, while in (d) the view is from underneath. The red spot in (d) corresponds to the equatorial n-pair; note that, for the resolution of colours employed, there is no corresponding red spot on the inside, under-surface for the axial n-pair. The equatorial red spot is also visible in (c). This indicates that the equatorial n-pair is more nucleophilic than the axial n-pair.
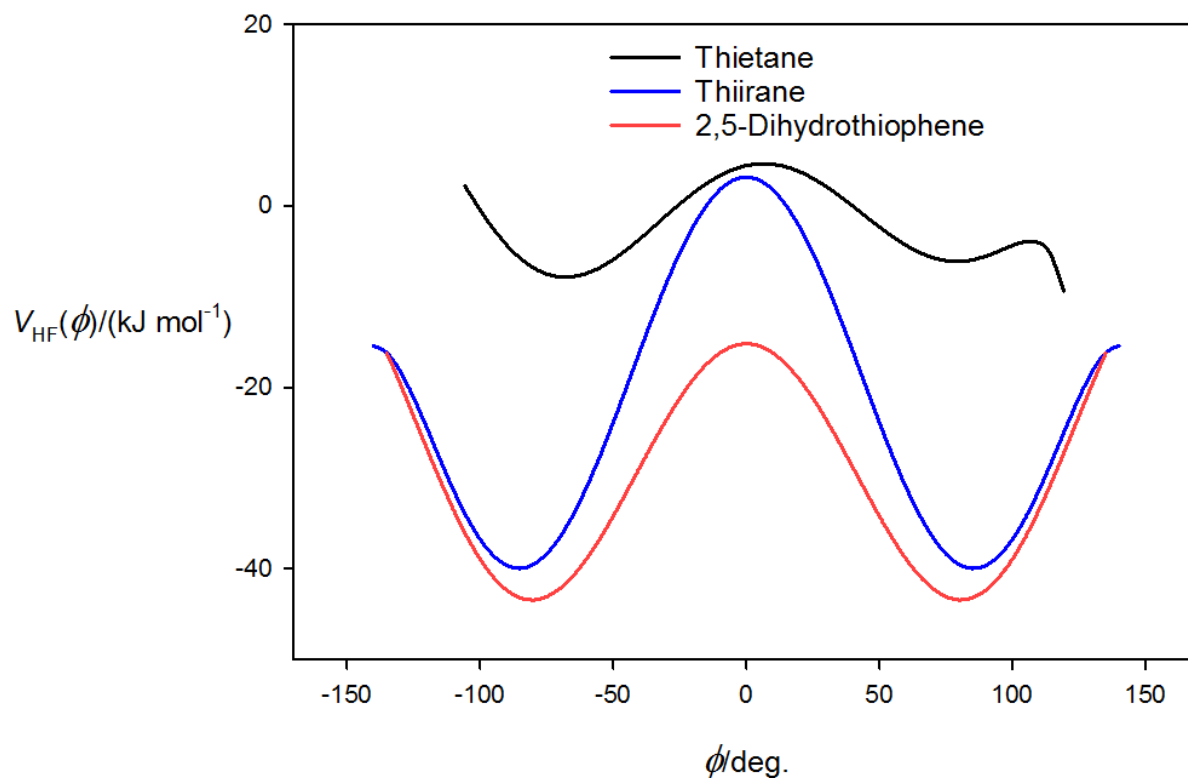
Figure 6. Plot of the potential energy $V(\phi)$ of the extended electric dipole model of HF (see text for model details) as a function of the angle ϕ made by the HF molecule at S with the C_2 axis (for thiirane and 2,5-dihydrothiophene) or the plane of S and its contiguous C atoms (thietane). The distances r of H from S are those given in the caption to Figure 4. For clarity, 15 kJ mol^{-1} has been added to each point of the thietane curve.
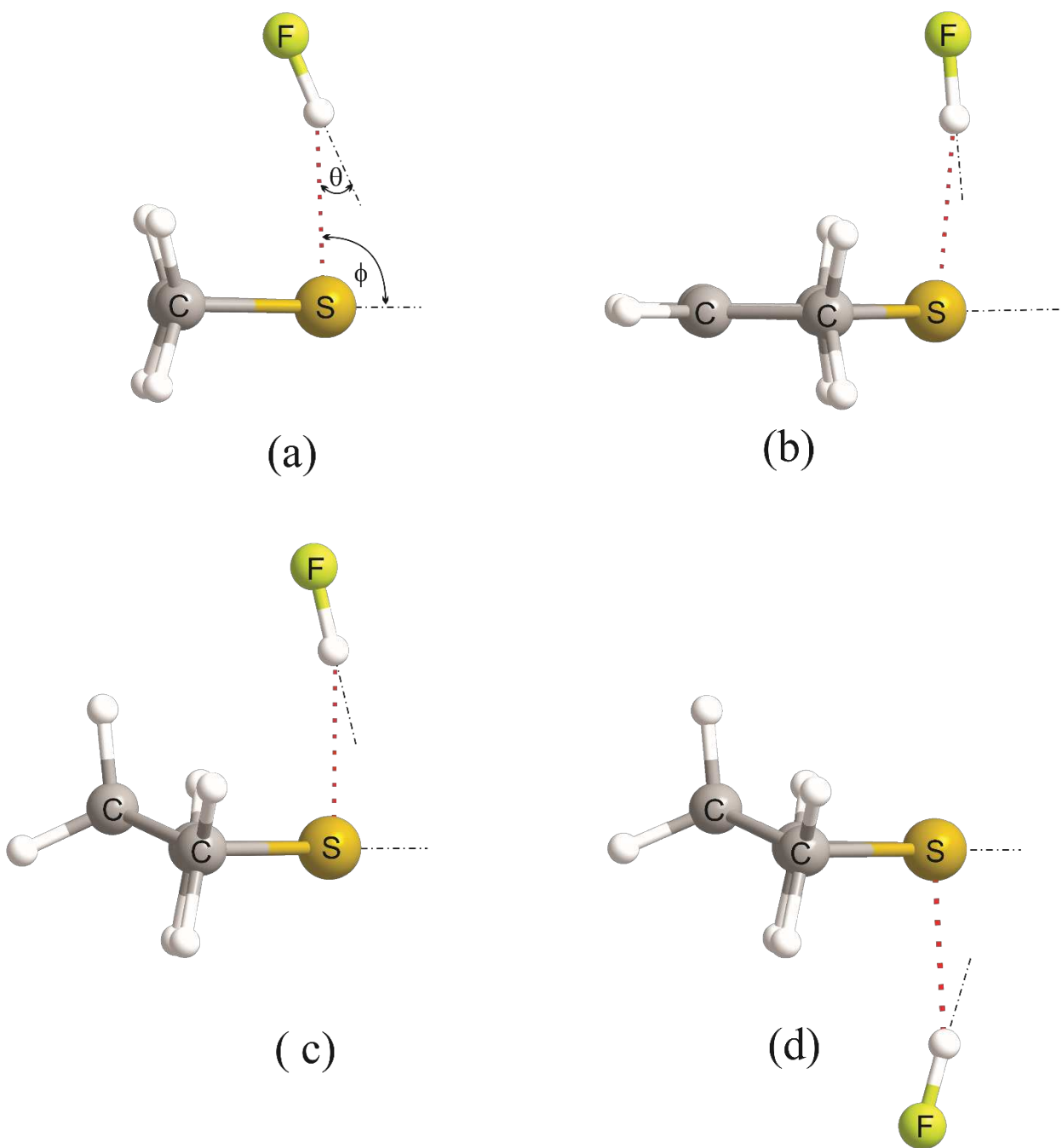
Figure 7. *Ab initio* geometries of (a) thiirane···HF, (b) 2,5-dihydrothiophene···HF, (c) the axial conformer of thietane···HF, and (d) the equatorial conformer of thietane···HF determined in optimisations carried out at the CCSD(T)-F12c/cc-pVTZ-F12 level of theory. Diagrams are to scale. The angles ϕ and θ [defined in (a)] are as follows: (a) $\phi = 93.1°$ and $\theta = 21.1°$, (b) $\phi = 84.5°$ and $\theta = 10.3°$, (c) $\phi = 88.5°$ and $\theta = 14.1°$, and (d) $\phi = 76.6°$ and $\theta = 17.5°$. Further geometrical details are available in the Supplementary Material. The energy difference of the axial (c) and equatorial (d) conformers of thietane···HF is 1.41 kJ mol^{-1} when calculated at the CCSD(T)-F12c/cc-pVTZ-F12 level.